A molecular design approach towards elastic and photopatternable polymer electronics

Yu Zheng^{1,2}†, Zhiao Yu^{1,2}†, Song Zhang³, Xian Kong¹, Wes Michaels¹, Weichen Wang^{1,4}, Gan Chen^{1,4}, Deyu Liu¹, Jiancheng Lai¹, Nathaniel Prine³, Weimin Zhang⁵, Shayla Nikzad¹, Chris B. Cooper¹, Donglai Zhong¹, Jaewan Mun¹, Jiheong Kang^{1,6}, Jeffrey B.-H. Tok¹, Iain McCulloch⁵, Jian Qin¹, Xiaodan Gu³, Zhenan Bao^{1*}

¹Department of Chemical Engineering and ²Department of Chemistry, Stanford University, Stanford, CA 94305, USA. ³School of Polymer Science and Engineering, The University of Southern Mississippi, Hattiesbury, MS 39406, USA. ⁴Department of Materials Science and Engineering, Stanford University, Stanford, CA 94305, USA. ⁵King Abdullah University of Science and Technology (KAUST), Kaust Solar Center (KSC), Thuwal 23955-6900, Saudi Arabia. ⁶Department of Materials Science and Engineering, Korea Advanced Institute of Science and Technology (KAIST), Daejeon 34141, Republic of Korea.

- † Yu Zheng and Zhiao Yu contributed equally to this work.
- * Corresponding author, e-mail: zbao@stanford.edu

Abstract

Next-generation wearable electronics will require enhanced mechanical robustness and complexity. Besides previously reported softness and stretchability, desired merits for realistic devices include high mobility, elasticity, solvent resistance and photo-patternability. However, each property requires a particular molecular design and has not been simultaneously achieved. Here, for the first time, we integrate all these targeted properties into both polymeric semiconductors and dielectrics, without comprising their electrical performance. This is enabled by a covalently-embedded, in-situ rubber matrix (iRUM) formation designed through excellent miscibility of iRUM precursors with both conjugated and insulating polymers; Additionally, controlled composite film morphology is paired with the beauty of azide chemistry. The high covalent crosslinking density resulted in remarkable elasticity and solvent resistance in both layers. When applied in fully stretchable transistors, the iRUM semiconductor film retains its charge carrier mobility even after stretching to 100% strain and exhibits a 1 cm² V⁻¹ s⁻¹ record-high mobility retention after 1000 stretching-releasing cycles at 50% strain. Furthermore, we fabricated a fully patterned elastic transistor array via consecutively photopatterning of dielectrics and semiconductors, demonstrating the feasibility of integrated solution-processed electronics manufacturing. Furthermore, the cost-effectiveness of iRUM precursors along with their high contents in active layers endow them with promise in mass production. The iRUM approach represents an important advance in molecule-level design for robust and multifunctional skin-inspired electronics.

Introduction

Skin-like electronics have garnered considerable interests over the past decade for their potential applications in robotics, prosthetics, health monitoring and medical implants.¹ Currently, stretchable electronics are made by either applying geometric designs on rigid inorganic-based devices using buckled substrates^{2,3} or developing intrinsically stretchable organic electronic materials.^{4,5} However, softness and stretchability reported before are still far from the requirements for realistic consumer electronics.⁶ High electrical performance combined with elasticity, solvent resistance, and facile patternability are desired merits but have not been possible concurrently.

Organic electronic materials, especially polymers, have been identified as promising candidates to realize stretchable electronics due to their structural tunability, solution processability, cost-effectiveness and high-density manufacturing. Albeit theoretically promising, the key components in organic electronics, i.e. semiconductors and dielectrics, still face many challenges. For integrated circuits, sensory array and display fabrication, the organic semiconductors and dielectrics need to be patterned through a simple yet universal solution-based deposition method. However, good solution processability is usually accompanied by poor solvent resistance. This is thus a 'mixed blessing' for organic electronic materials, since it results in good solution processability but suffers from chemical erosion during the solution-processed fabrication of multilayer devices, limiting the possibility of low-cost and scalable production. Frequently, transfer methods are employed, which result in increased complexity and cost as well as low device yield, making it challenging to produce complex device and scale up. Furthermore, many previously reported electronic materials are viscoelastic, causing unreliable hysteresis performance when subjected to harsh mechanical challenges, e.g. multiple, high-loading stretching-releasing cycles. 10

Developing an elastic semiconductor without sacrificing electrical performance remains a desired objective but particularly challenging. Conjugated polymers are promising due to their chemical versatility and potential mechanical flexibility, but most of them still experience device failure under low strain due to their semicrystalline thin film morphology. Essentially all previously reported molecular design rules focused on increasing the 'stretchability', i.e. enhancing the ultimate fracture strains of polymer semiconductors without loss of electronic functionalities, in which 'reducing long-range crystalline order' has been the general principle. However, the semiconductor film in these cases always suffers from unreversible permanent plastic deformation prior to crack formation. Upon removal of strain, the semiconductor film supported on an elastic dielectric tends to form wrinkling and buckling. Unfortunately, these processes invariably lead to interfacial delamination and degrade charge transport. For practical applications, the semiconductor needs to function after many strain cycles, and thus elasticity beyond simple stretchability while maintaining high charge transporting ability is highly demanded for stretchable polymer electronics. This requires high covalent crosslinking density as well as chain flexibility in active layer, while balancing sophisticated charge transport over multiple length scales.

Patterning is another critical aspect for practical polymer electronics. Previous reports include protection-etching patterning method that required multiple steps involving sacrificial layer and orthogonal chemicals¹⁶ and inkjet printing that has difficulties in producing uniform devices.¹⁷ To achieve facile patternability as well as chemical robustness, photo-patterning using crosslinking chemistry is known to be a clever approach, which requires covalent bonding between crosslinkers and organic electronic materials.^{18,19} However, introducing crosslinkers usually results in a higher elastic modulus and lower fracture strain even as compared to pristine semiconductors and dielectrics.¹⁸ Limited examples of rationally designed crosslinkers were observed to

increase the fracture strain of semiconductors; unfortunately, they all significantly degraded the charge carrier mobility at a mere 5 w.t. % addition due to the disruption of semiconductor aggregation, and the materials still exhibited viscoelastic behavior.^{20,21} Another reported approach was blending a polymer semiconductor with an elastomeric polymer; however, the high percentage of elastomers in the film's composition rendered the film even more susceptible to the corrosive organic solvents, even though they exhibited relatively stable electrical performance under mechanical deformation^{22–24}. For dielectrics, some fluorinated elastomers were designed to be organic solvent resistant, but they either showed double-layer capacitive effect,²⁵ or relied heavily on surface-modification to achieve suitable wettability for semiconductor solution deposition.¹⁷ Thus far, no reported general molecular design approach can simultaneously achieve elasticity and photo-patternability while not degrading electrical performance for polymer electronic materials.

Design Principles of iRUM Approach

Here, we report rationally designed single precursors for covalently-embedded in-situ rubber matrix (iRUM) formation, which can undergo both self-crosslink and crosslink with corresponding electronic materials in elegantly controlled ratio, thus achieving all targeted properties for both polymeric semiconductors (**PSC**) and dielectrics (Fig. 1a).

Briefly, for semiconductors, an iRUM precursor consisting of perfluorophenyl azide (PFPA) end-capped polybutadiene, **BA** (Supplementary Information Synthetic Methods), was designed and formed to enable the following *key* features:

- (i) the highly flexible backbone structure and compatible surface energy (30.4 mJ/m²) of **BA** enabled its excellent miscibility with **PSC** (30-33 mJ/m²), thus allowing for high crosslinking density;
- (ii) **BA** was found to undergo self-crosslink to generate a stretchable and elastic matrix through azide/C=C cycloaddition²⁶ (Supplementary Scheme. 1), improving both stretchability and elasticity of the 'semiconductor-in-rubber' film;
- (iii) the azide groups of **BA** also reacted with and crosslinked the alkyl chains on polymer semiconductors through azide/C–H insertion²⁷ (Supplementary Scheme. 1), ensuring the solvent-resistance and photopatternability;
- (iv) a much higher proportion of **BA** underwent self-crosslink described in (ii) since the reactivity of cyclization is seven times faster than that of azide/C–H insertion.^{28,29} This leads to finely controlled competition between forming a rubber matrix and crosslinking **PSC**, allowing for maintained charge transport pathway.

With these features, this as-formed elastic matrix was found to be uniformly embedded into **PSC** network via controlled covalent bonding. Moreover, hydroxyl-terminated polybutadiene is a widely utilized ingredient in rubber industry for nearly a century and is available in low-cost and large-scale.³⁰

For dielectrics, an iRUM precursor consisting of perfluorophenyl azide (PFPA) end-capped hydrogenated-polybutadiene, **BH** (Fig. 1a and Supplementary Information Synthetic Methods), was designed for a widely-used stretchable dielectric material, polystyrene-block-poly(ethylene-co-butylene)-block-polystyrene (**SEBS**). The vastly increased crosslinking density between the as-formed rubber matrix and dielectrics is critical to realize elasticity, and provides remarkable solvent resistance which is necessary for direct depositing and photopatterning of semiconductors on top.

Two key breakthroughs of iRUM are demonstrated and proved later in the paper:

(i) Different from conventional stretchable polymer semiconductors, the iRUM approach results in the *first* molecular-level intrinsically elastic semiconductor without comprising charge carrier mobility (Fig. 1b). (ii) *For the first time*, the iRUM approach achieves the integration of all desired merits for polymer electronic materials, from both daily use and manufacturing perspectives (Fig. 1c).

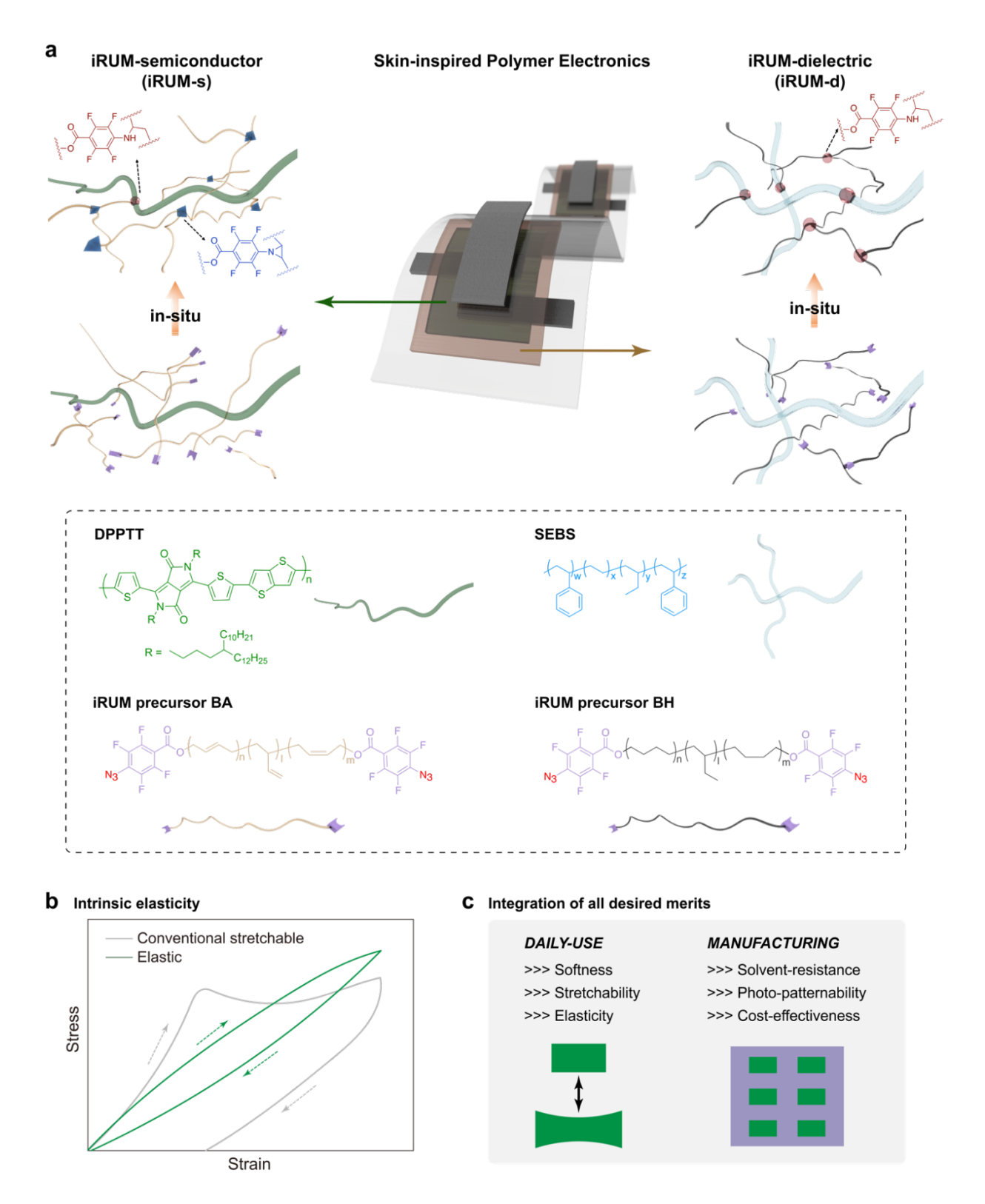


Fig. 1. Schematic illustration of iRUM approach for both semiconductors and dielectrics. (a) For semiconductors, DPPTT network is covalently embedded into the in-situ formed elastic rubber matrix generated

by iRUM precursor **BA**. In iRUM-s, the number of crosslinking sites created through azide/C=C cycloaddition is much higher than that created through azide/C-H insertion. For dielectrics, **SEBS** is uniformly crosslinked by iRUM precursor **BH** through azide/C-H insertion. The good miscibility between iRUM precursors and DPPTT/SEBS significantly improves the crosslinking density in both semiconductor and dielectric layers. (**b**) Conceptual cyclic stress-strain curves of conventional stretchable **PSC** and elastic **PSC** demonstrated in this work. Conventional stretchable **PSC** undergoes plastic deformation, with residue strain left after one single loading-unloading cycle. When such a semiconductor film is supported on an elastic dielectric, the as-formed wrinkling and buckling lead to interfacial delamination, and significantly degrade charge transport. The elastic **PSC** can return to its original length after strain released, which contributes to more stable semiconductor/dielectric interface under cyclic strains. (**c**) iRUM approach achieves the integration of all desired merits for skin-inspired polymer electronics from both daily use and manufacturing perspectives, without comprising electrical performance.

Applying iRUM Approach in Polymer Semiconductors

Rationally designed precursor family and matrix formation

We first investigated the iRUM approach in semiconductors. In order to rationalize the molecular design principles of **BA** (Fig. 2a), we synthesized different polybutadiene-based precursors (Supplementary Information Synthetic Methods):

- (i) polybutadiene-fluorine (**BF**) that is structurally similar to **BA** but cannot crosslink (Fig. 2b),
- (ii) polybutadiene-acrylate (**BAc**) that can only undergo self-crosslink to form an elastic rubber network, but no covalent crosslink with **PSC** (Fig. 2c), and
- (iii) polybutadiene-hydrogenated-azide (**BH**) which serves as a reference to compare the effect of reactivity difference between azide/C–H insertion and azide/C=C cycloaddition on the semiconductor electrical performance (Fig. 2d).

As described above, we observed that the iRUM precursor **BA** can react with its own C=C bonds to form an elastic rubber matrix. It showed no residue strain left behind after repeated stretching-releasing cycles (Fig. 2e, Supplementary Fig. 1). Next, we chose a widely-used high mobility donor-acceptor (D-A) conjugated polymers, poly-thieno[3,2-b]thiophene-diketopyrrolopyrrole (**DPPTT**) (M_n: 62.7 kg/mol, PDI: 2.9) as a model semiconductor to investigate the feasibility of our approach. The obtained semiconductor film is named 'iRUMs-x:y', in which 's' stands for semiconductor and 'x:y' is the BA-to-DPPTT weight ratio. As observed from atomic force microscopy (AFM), iRUM-s-3:7, -1:1, and -3:1 all exhibited uniform morphology (Fig. 2f, Supplementary Fig. 2) and low surface roughness (1.8-2.4 nm), even though the weight of **BA** is up to three times that of **DPPTT**. Additionally, the composition map of the film surface obtained through atomic-force microscopy paired with infrared spectroscopy (AFM-IR) further confirmed the well-dispersed DPPTT network within the continuous BA-formed rubber matrix (Fig. 2f, Supplementary Fig. 3). Molecular dynamics (MD) simulations of BA/DPPTT blending systems further confirmed their uniform mixing, and suggests a stronger association between BA and DPPTT side chains than that between BA and DPPTT backbone (Fig. 2g, Supplementary Fig. 4 and 5). The uniform mixing between BA and polymer semiconductor serves as the key premise in ensuring high crosslinking density. Similarly, the blended or crosslinked **DPPTT** films with **BF**, BAc or BH all exhibited uniform mixing (Supplementary Fig. 6 to 11). This excellent miscibility originates from the surface energy match between the two components and relatively low molecular weight of BA. Furthermore, the BA and BH are highly flexible polymers, and therefore, a strong decrease of free energy is expected from entropy gain of mixing. 31,32 The low packing tendency of polybutadiene backbone also excludes the possibility of enthalpy gain through suppressing crystallization (Supplementary Note 1).

Maintained electrical performance

The electrical performance of iRUM-s-x:y films were characterized in bottom-gate top-contact transistors with highly-doped Si as a gate electrode, MoO₃/Au as source and drain electrodes and octadecyltrimethoxysilane (OTS)-modified SiO₂ as dielectrics. As shown from transfer curves and extracted charge carrier mobilities (Fig. 2h and 2i, Supplementary Fig. 12), this iRUM approach did not adversely affect the electrical performance of semiconductors, with all mobilities being maintained at ~1 cm² V⁻¹ s⁻¹ for different **BA** proportions. We hypothesized that this was due to the well-controlled ratio of C=C cycloaddition (i.e. reaction between azide and polybutadiene backbone), versus C-H insertion, (i.e. reaction between azide and side chains on polymer semiconductor during crosslinking), as confirmed later. Since the charge carrier mobilities in BF/DPPTT blend films (Fig. 2b) and BAc/DPPTT crosslinked films (Fig. 2c) were also unaffected, it indicates that blending with polybutadiene precursors and the in-situ elastic rubber matrix formed inside the polymer semiconductor network will not disrupt the charge transport pathways (Fig. 2h, Supplementary Fig. 13 and 14). On the contrary, the mobility was observed to suffer a drastic decay in **BH/DPPTT** crosslinked films, from 1 cm² V⁻¹ s⁻¹ for pristine **DPPTT** to 0.12 cm² V⁻¹ s⁻¹ for **BH/DPPTT**-1:1 further to 0.06 cm² V⁻¹ s⁻¹ for **BH/DPPTT**-3:1, as the **BH** concentration increases (Fig. 2h and 2i, Supplementary Fig. 15). To better understand this drastic difference, we performed multiple morphological characterizations. As revealed by the depth profiles of X-ray photoelectron spectroscopy (XPS), the semiconductor component in both iRUM-s-1:1 and BH/DPPTT-1:1 crosslinked film showed a similarly uniform distribution across film thickness (Supplementary Fig. 16 to 20). Therefore, the difference in electrical performance cannot be simply explained by different vertical distribution of DPPTTs.

Based on the above observations, we hypothesize that the difference in reactivity may be contributing. **BA** may mostly have reacted with its double bonds to create a rubber matrix, instead of reacting with the side chains of semiconductor that will disrupt chain packing and aggregation, thus able to maintain its charge transport pathway. The higher reactivity of azide/C=C cycloaddition than that of azide/C-H insertion is supported by thermogravimetric analysis (TGA) and attenuated total-reflectance Fourier transformation infrared spectroscopy (ATR-FTIR) (Supplementary Fig. 21 and 22). Different from **BA**, the all-single-bond backbone on **BH** is chemically indistinguishable with the long side chains on semiconductors, resulting in their equal reactivity with azides and potentially more disruption of the semiconductor aggregation.²¹ This is supported by ultraviolet-visible absorption spectra (UV-vis) results. Specifically, the semiconductor aggregation in **BAc/DPPTT** and **BA/DPPTT** (iRUM-s) slightly increased in crosslinked films compared to their simply blended films without crosslinking; while on the contrary, a clear decrease in aggregation was observed in **BH/DPPTT** films after crosslinking (Fig. 2j, Supplementary Fig. 23 and 24). Additionally, as indicated by grazing-incidence X-ray diffraction (GIXD), the edge-on crystalline domain size slightly increased in iRUM-s-x:y films compared with the neat **DPPTT** film, while the mean crystallite size decreased in **BH/DPPTT** crosslinked films (Supplementary Fig. 25 to 28, Table 1 to 4, Note 2).

Softness and stretchability

Next, the stretchability of iRUM-s-x:y was studied by applying various levels of strain on a polydimethylsiloxane (PDMS)-supported thin film.³³ For iRUM-s-1:1, and -3:1, they can be stretched up to 100% strain without showing any visible cracks. In contrast, neat DPPTT film showed dense and micrometer-scale cracks at 100% strain (Fig. 2k, Supplementary Fig. 29). Furthermore, pseudo free-standing tensile tests were performed by floating the semiconductor film on water, which provided characterization of intrinsic thin-film mechanics.^{34,35} From our obtained stress-strain curves, the iRUM-s-3:1 film exhibited nearly one-order-of-magnitude increase in fracture strain and four-time decrease in elastic modulus compared to neat film (Fig. 21,

Supplementary Fig. 30). This significant improvement in stretchability and softness originates from the increased proportion of the rubber matrix created by **BA**, which has a much lower elastic modulus (6.9 MPa) and higher fracture strain (145.9 %) than that of pristine **DPPTT** (464.9 MPa and 4.5 %, respectively) (Supplementary Fig. 1 and 30). When such an iRUM-s film undergoes mechanical deformation, the in-situ-formed crosslinked matrix provides stretchability and elasticity. Without crosslinking, the blend film of **BF/DPPTT** exhibited a decreased elastic modulus than neat **DPPTT** film, as expected from the plasticizing effect of the polybutadiene. However, its fracture strain is still as low as 3.9 % and cracks still formed at 50 % strain despite reduced crack sizes. The other two types of semiconductor films with crosslinked matrixes, **BAc/DPPTT**-1:1 and **BH/DPPTT**-1:1, also showed both improved softness and stretchability than the neat film (Fig. 2m, Supplementary Fig. 31 and 32).

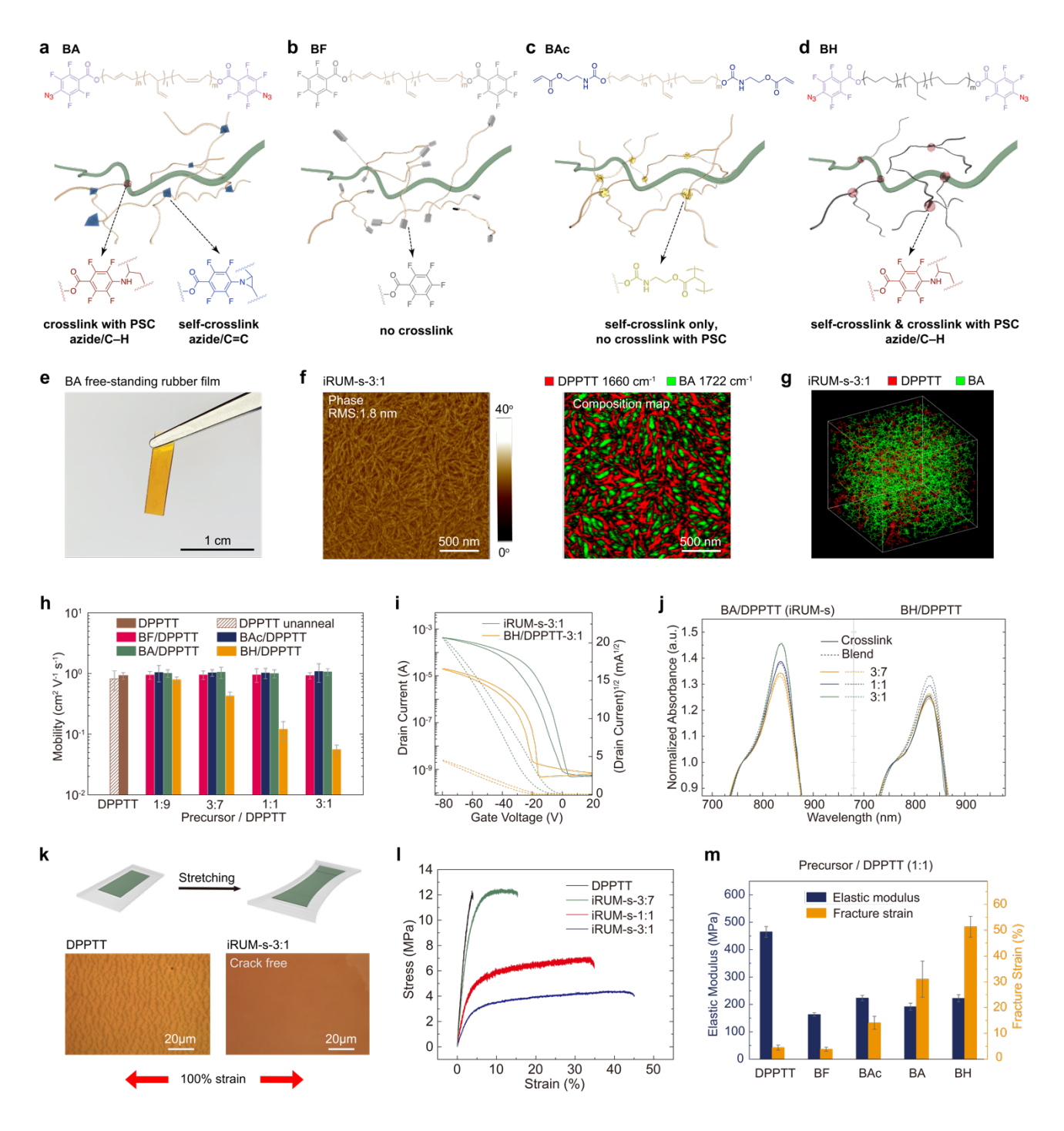


Fig. 2. Systematic investigation of molecular design principles of iRUM semiconductors. The obtained semiconductor film is named 'iRUM-s-x:y', in which 's' stands for semiconductor and 'x:y' is the BA-to-DPPTT weight ratio. Chemical structures of different polybutadiene-based precursors (a) BA, (b) BF, (c) BAc, (d) BH, and the generated semiconductor film after blending with DPPTT followed by thermal annealing at 150 °C. (e) The free-standing elastic rubber film created by BA through azide/double bond cycloaddition. (f) AFM phase image and AFM-IR overlay image of iRUM-s-3:1 film. The surface roughness is obtained from AFM height image. In the composition map, red color represents **DPPTT** phase probed by IR laser at 1660 cm⁻¹ and green color represents **BA** phase probed at 1722 cm⁻¹ respectively. (q) Screen shot of MD simulated iRUM-s-3:1 film (simulation box length: ~5.8 nm), showing distributions of **DPPTT** and **BA** in a blend. (h) The extracted mobility of iRUM-s-x:y (BA/DPPTT-x:y) films, BF/DPPTT-x:y blend films, BAc/DPPTT-x:y and BH/DPPTT-x:y crosslinked films where x:y is the precursor-to-DPPTT weight ratio, characterized in bottom-gate top-contact transistors using SiO₂ (300 nm)/Si as dielectric and gate electrode. (i) The representative transfer curves for iRUM-s-3:1 and BH/DPPTT-3:1 films. (j) UV-vis spectrum for iRUM-s and BH/DPPTT films prior and after thermal crosslinking. (k) Schematic illustration of the stretching of semiconductor film on a supported PDMS substrate. Optical microscope images of a neat DPPTT film and an iRUM-s-3:1 film under 100% strain. (I) The representative stress-strain curves for **DPPTT** and iRUM-s-x:y films obtained from pseudo free-standing tensile tests. 34,35 (m) The extracted elastic modulus and fracture strain of iRUM-s (BA/DPPTT) films, BF/DPPTT blend films, BAc/DPPTT and BH/DPPTT crosslinked films obtained from pseudo free-standing tensile tests (the precursor-to-DPPTT weight ratio is 1:1).

Fully stretchable transistors and intrinsic elasticity

We proceeded to fabricate fully stretchable transistors to evaluate the electrical performance of iRUM-s under mechanical deformation, with carbon nanotube (CNT) as gate and source/drain electrodes and PDMS as dielectrics (Fig. 3a). As shown in a representative transfer curve, iRUM-s film showed ideal and comparative transistor performance as neat film, with an average mobility of 0.5 cm² V⁻¹ s⁻¹ (Fig. 3b). The decreased mobility compared to that obtained from a rigid transistor originates from higher contact resistance of CNT than Au electrode. The mobility was stably maintained despite the device being stretched up to 100 % strain along the charge transport direction, while the neat film exhibited dramatic mobility degradation (Fig. 3c, Supplementary Fig. 33). As pointed out before, practical electronic device needs to reliably operate beyond a single stretching and maintain its functionalities under harsh cyclic loading. Therefore, we performed cyclic tests on the transistor at 50 % strain (higher than typically applied strains needed for skin-inspired electronics, i.e. ~20-30 %). The iRUM-s film showed remarkably stable charge carrier mobility (0.3 cm² V⁻¹ s⁻¹) and on current even after 1000 stretching-releasing cycles under strain released state (Fig. 3d, Supplementary Fig. 34 and 35). This excellent cyclic durability was attributed to the robust elasticity of composite semiconductor film enabled by our iRUM approach.

To confirm our obtained elasticity improvement, we next performed mechanical tests for a bilayer specimen where an iRUM-s film (35 nm thick) was supported on a thin PDMS substrate (2.4 µm thick). A recent report demonstrated the feasibility of this film-laminated-on-thin-elastomer approach to measure the viscoelastic behavior of a conjugated polymer thin film under large cyclic strains.³⁷ The viscoelasticity of conjugated polymer film was then extracted from the measurement on the bilayer structure and was found to significantly impact film stability after cycling. For our iRUM-s-3:1 film which was used in stretchable transistors, the stress-strain curves with increasing cyclic strains from 10 % to 70 % showed no residual strain upon strain removal (Fig. 3e). By contrast, the iRUM-s-3:7 film exhibited a ~4 % residue strain due to lower rubber matrix content and thus slight plastic deformation (Fig. 3f), which is consistent with the observation of wrinkle formation after repeated stretching cycles observed via AFM (Supplementary Fig. 36). Furthermore, iRUM-s-3:1 film showed less stress relaxation and a much-reduced hysteresis (Supplementary Fig. 37 and 38), indicating the transition from viscoelasticity to entropy-driven fully elastic behavior.³⁸ When such a semiconductor film is stretched, the

strain energy can be dissipated through conformational change of the in-situ formed rubber matrix, while the covalent crosslinking sites provide the film with 'rebound force' to return to its original state. The underlying mechanism was further cross-validated by the existence of residue strain and higher hysteresis as obtained from cyclic tests of **BF/DPPTT-3**:1 blend film and **BAc/DPPTT-3**:1 crosslinked film (Supplementary Fig. 39 and 40). To the best of our knowledge, this is *the first and direct demonstration* of the elastic behavior of polymer semiconductor film under cyclic mechanical testing.

To examine the versatility of our iRUM approach, we applied it to another high-mobility D-A conjugated polymer, indacenodithiophene-co-benzothiadiazole (IDTBT)³⁹ (M_n: 104.5 kg/mol, PDI: 2.8). Different from semicrystalline **DPPTT**, **IDTBT** is known to exhibit a quasi-amorphous morphology and low energetic disorder. We previously reported that **IDTBT** exhibited high stretchability (crack on-set strain >100 % when supported on a PDMS substrate) but poor cyclic durability due to plastic deformation, as confirmed by clear wrinkle formation and sharp mobility decrease (from >1 down to 0.07 cm² V⁻¹ s⁻¹) after 500 stretching-releasing cycles at 50 % strain. Transforming such a poor-cycling semiconductor to elastic one is meaningful yet challenging. After applying iRUM approach on IDTBT with BA/IDTBT ratio of 3:7, the previously observed wrinkle formation for neat IDTBT after repeated stretching cycles were completely eliminated. The average mobility was maintained at >1 cm² V⁻¹ s⁻¹ even after 500 loading-unloading cycles at 50 % strain under strain released state in fully stretchable transistors (Fig. 3g and 3h, Supplementary Fig. 41 to 45). This is a record-high mobility retention (as compared to all other strategies reported in the literature thus far), and the applied cyclic strain level (50%) is two times higher than conventional strain level, i.e. 25 %, used in most of the reported systems 40-⁴³ (Fig. 3i). As a comparison, we observed poor cyclic durability for un-crosslinked **BF/IDTBT** blend film, thus confirming again the elastic property of iRUM-IDTBT is the critical factor for the stable cycling performance rather than only modulus match or interfacial crosslinking with dielectrics (Supplementary Fig. 46 and 47). Furthermore, we observed the stretchability of iRUM-IDTBT film was maintained while exhibiting an increased softness (reduced elastic modulus), as confirmed by pseudo free-standing tensile tests and crack on-set strain characterizations (Supplementary Fig. 48 and 49).

Interfacial crosslinking

The accessible C=C double bonds of **BA** backbone located on the surfaces of iRUM-s film provide additional opportunities to engineer the semiconductor-dielectric interface. These double bonds are able to undergo various chemical reactions, e.g. hydrosilylation with silicon-hydride (Si–H), thiol-ene reaction with S–H group, ⁴⁴ and cycloaddition with azide. We reasoned that interfacial crosslinking can be created between **BA** rubber and PDMS through Si–H/vinyl reactions during curing process, as evidenced by a much higher interfacial toughness obtained from 180° peeling tests when compared to PDMS/PDMS interface⁴⁵ (Fig. 3j). We observed that the PDMS portion fractured even before the breakage of **BA**/PDMS interface, while two pieces of PDMS can be readily separated (Supplementary Fig. 50, Video 1). Such strong interfacial interaction ensures good adhesion and prevents delamination between semiconductor and dielectric, which is beneficial for stable cyclic operation of electronic devices.

Solvent-resistance and photo-patternability

The chemical crosslinking nature of the iRUM approach provides solvent resistance for polymer semiconductors, which is necessary for multilayer device fabrication. After treating a crosslinked iRUM semiconductor film with various organic solvents, such as trichloroethylene, chloroform, chlorobenzene and toluene which are commonly used to process polymer semiconductors, the surface remained smooth with low

roughness (~1.7 to 1.8 nm) indicating little material being dissolved away by solvent. In addition, the morphology was well-maintained as observed from both height and phase images by AFM (Fig. 3k). This observation was attributed to the covalent bonding between the in-situ formed **BA** rubber and polymer semiconductor network. On the other hand, **BAc/DPPTT** crosslinked film and **BF/DPPTT** blend film were found to be either partially or totally removed after organic solvent treatment due to the lack of covalent binding with **DPPTT** (Supplementary Fig. 51). Besides solvent resistance, we reasoned that since the crosslinking reaction of azide group can be activated by UV light, our iRUM approach can be used to photo-pattern polymer semiconductors. Through selective UV exposure (254 nm for 1 min), the photo-crosslinked regions of iRUM-s film will be immobilized, while the non-crosslinked regions can subsequently be 'washed away' using appropriate organic solvents (Fig. 4a). More importantly, no degradation was observed in electrical performance of the RUM-s film during photo-crosslinking and chloroform solvent development process. As a result, the photo-patterned semiconductor film exhibited equivalently high mobility compared with neat film, achieving an averaged mobility of 1.05 cm² V⁻¹ s⁻¹ for a 10×10 transistor array (Fig. 4b and 4c).

Our results underscored the following molecular design guidelines towards multifunctional **PSC**, which are: (i) uniform mixing of rubber matrix precursors with conjugated polymers is the premise of high covalent crosslinking density, (ii) stretchability and elasticity can be achieved through the as-formed crosslinked rubber matrix, (iii) covalent crosslinking between precursor and **PSC** is necessary for solvent-resistance and photopatternability, and (iv) the composite film morphology needs to be finely controlled through balancing the process of forming a rubber matrix and crosslinking **PSC**, in order to maintain charge transport.

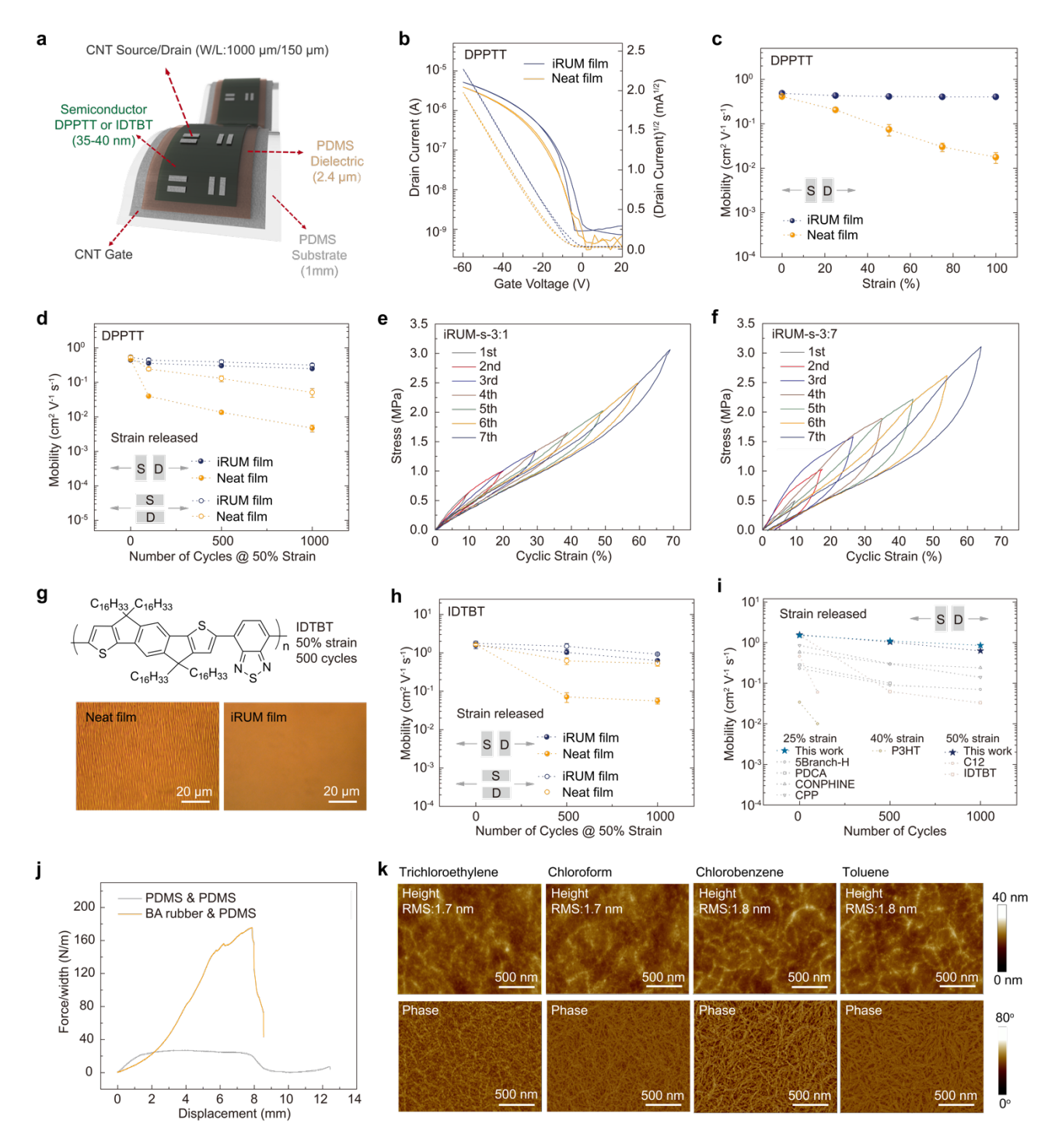


Fig. 3. Characterization of the electrical performance of iRUM-s under mechanical deformation and solvent resistance. (a) Device structure of a fully stretchable transistor with a bottom-gate top-contact configuration, W/L = 1000 μ m/150 μ m . (b) Representative transfer curves of a stretchable transistor with neat DPPTT film or iRUM-s as the semiconductor. (c) Evolution in mobility at different strains during single stretching, with charge transport parallel to stretching direction. (d) Evolution in mobility after multiple stretching-releasing cycles at 50 % strain under strain released state, with charge transport parallel and perpendicular to stretching direction. Stress-strain curves with a cyclic strain range of 10-70 % for (e) iRUM-s-3:1 and (f) iRUM-s-7:3 films. (g) Curves of the peeling force per width of PDMS sheet versus displacement for BA rubber and PDMS. The higher peeling force between BA rubber and PDMS indicates the formation of interfacial crosslinking. (h) Optical microscope images of IDTBT and iRUM-IDTBT after 500 stretching-releasing cycles at 50 % strain. (i) Changes in mobility of a neat IDTBT film and an iRUM-IDTBT film after multiple stretching-releasing cycles at 50% strain under strain released state. (j) Comparison of the cyclic durability in this study with previously reported results

in the literature^{40–43} (spin-coated semiconductor films using insulating polymer dielectrics under strain released state without applying other engineering techniques, which reflects the intrinsic properties of semiconductors). (**k**) AFM height and phase images of iRUM-s-3:1 after soaking in various organic solvents (trichloroethylene, chloroform, chlorobenzene and toluene) for 30 s. The surface roughness is extracted from AFM height image.

Applying iRUM Approach in Polymer Dielectrics

Besides polymer semiconductors, we further applied our iRUM approach to a high-performance dielectric material, polystyrene-block-poly(ethylene-co-butylene)-block-polystyrene (SEBS). Previously reported crosslinked SEBS was still easily swelled during consecutive deposition of other organic layers. 17 Direct solution-based deposition of semiconductors on top of dielectrics is an industry-friendly process yet longstanding issue in this field, so we test the iRUM strategy to address the above limitation. BH was chosen as the precursor to maximize the number of covalent crosslinking sites with SEBS (as elaborated above, BA tends to react more with itself while BH has equal reactivity with both SEBS and itself) and to avoid current-voltage hysteresis that may arise from C=C as traps in the polybutadiene backbone. 46,47 The obtained dielectric is named 'iRUM-d-x:y', where 'd' stands for dielectric and 'x:y' is the BH-to-SEBS weight ratio. BH exhibited excellent miscibility with SEBS, without large-domain phase separation occurring until BH/SEBS = 1:1 (Supplementary Fig. 52). The iRUM-d film was measured to have a similar dielectric constant as SEBS (2.1-2.2) (Supplementary Fig. 53). To examine the solvent resistance of iRUM-d films, surface roughness characterization by profilometer before- and after-solvent treatment was conducted (Fig. 4d, Supplementary Fig. 54). iRUM-d-4:5 film remained smooth and uniform after depositing chlorobenzene or chloroform, with almost no change in roughness (~3 nm). In contrast, pristine SEBS film showed substantial swelling after solvent treatment, with roughness increased from 7 nm to 178 nm.

Next, we fabricated bottom-gate top-contact transistors with iRUM-s directly deposited and photo-patterned on top of iRUM-d (highly doped Si as gate and MoO₃/Au as source and drain electrodes). We observed that increasing the amount of **BH** in the crosslinked dielectric resulted in an increased charge carrier mobility of photo-patterned iRUM-s, with an averaged value of 0.8 cm² V⁻¹ s⁻¹ when using iRUM-d-4:5, and the transistor exhibited ideal transfer characteristics with low hysteresis (Fig. 4e and 4f, Supplementary Fig. 55, Table 5). This condition was harsher than that encountered during simple spin-coating or inject-printing process using semiconductor solution, as the materials need to survive multiple solvent washing steps. Notably, no further surface modifications on iRUM-d were needed to achieve desired uniform iRUM-s semiconductor film. Through increasing the covalent crosslinking density of dielectrics due to its excellent miscibility with iRUM precursor, we have addressed its rapid swelling issue upon solvent treatment. Additionally, despite significantly increased crosslinking density of SEBS, the iRUM-d film showed negligible changes in fracture strain and, in fact, a 50% decrease in elastic modulus. As observed from stress-strain curves (Fig. 4g and 4h), iRUM-d (1.2 μm thick) exhibited strain-hardening behavior and reduced hysteresis from cyclic mechanical testing as compared to pristine SEBS (Supplementary Fig. 56), underscoring the iRUM-d strong elasticity.

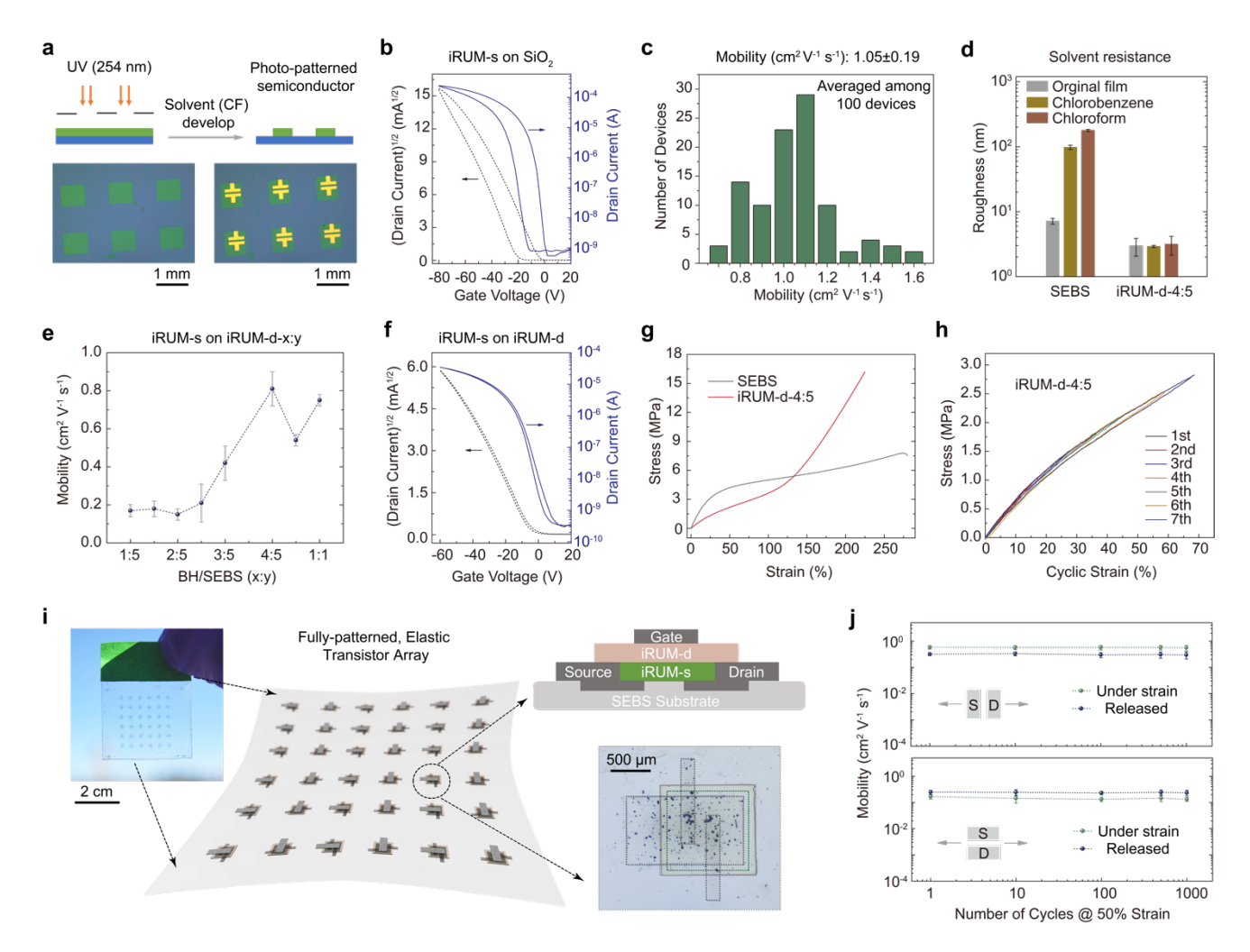


Fig. 4. The photo-patternability of iRUM-s and iRUM-d, and the integrated fully-patterned elastic transistor array. (a) Schematic illustration of the photo-patterning process for iRUM-s, which involves selective UV exposure and chloroform development. Optical microscope images of photo-patterned iRUM-s film (thickness: 35 nm) before and after depositing MoO₃/Au (2 nm/55 nm) electrodes. (b) A representative transfer curve of iRUM-s film that is photo-patterned on OTS-modified SiO₂ (300 nm) as characterized in a bottom-gate top-contact transistor. (c) Mobility distribution of photo-patterned iRUM-s from a 10×10 transistor array, with bottom-gate top-contact configuration, highly-doped Si as gate electrode, MoO3/Au as source/drain electrodes (W= 500 μm, L= 50 μm) and octadecyltrimethoxysilane (OTS)-modified SiO₂ (300 nm) as dielectrics. (d) Surface roughness characterization of SEBS and iRUM-d-4:5 films by profilometer before- and after-solvent treatment. (e) The mobility of photo-patterned iRUM-s film on iRUM-d-x:y (1-1.5 µm thick), where x:y is the BH-to-SEBS weight ratio. (f) A representative transfer curve of a bottom-gate top-contact transistor with iRUM-s directly photo-patterned on iRUM-d-4:5 (1µm thick). (q) The representative stress-strain curves for SEBS and iRUM-d-4:5 films obtained from pseudo free-standing tensile tests. (h) Cyclic stress-strain curves (10-70 % strains) for iRUM-d-4:5. (i) Schematic of a fully patterned, intrinsically stretchable and elastic transistor array. Twodimensional diagram showing the side view of transistor structure. (j) Changes in mobility for the patterned transistor array after multiple stretching-releasing cycles at 50% strain, with charge transport parallel and perpendicular to stretching direction.

Fully-patterned Elastic Transistor Array

Finally, iRUM-d can be successfully photo-patterned by UV (254 nm) exposure and solvent development (Supplementary Fig. 57 to 59). We have accordingly incorporated iRUM-s and iRUM-d into a fully-patterned elastic transistor array, which serves as the building-block elements in functional circuits for signal processing

and computation,⁴⁸ thus demonstrating the feasibility of integrating these newly developed materials and producing realistic skin-inspired electronics (Fig. 4i). Specifically, iRUM-d film was first photo-patterned on top of a water-soluble sacrificial layer poly(sodium-4-styrene sulfonate) (PSSNa).⁴⁹ Next, iRUM-s was directly spin-coated and photo-patterned on the top of iRUM-d, greatly simplifying the conventional protection-etching process for patterning semiconductors.¹⁶ This takes not only the advantages of the photo-patternability of iRUM-s, but also the chemical robustness of iRUM-d, which makes it compatible with layer-by-layer solution deposition during device fabrication. After patterning the CNT source and drain electrodes, laminating substrate, releasing device in water, and patterning CNT gate electrodes, we obtained the transistor array with an average charge carrier mobility of 0.5 cm² V⁻¹ s⁻¹ and a high mobility retention after 1000 stretching-releasing cycles at 50 % strain (Fig. 4j, Supplementary Fig. 60 and 61). Obtained cyclic stress-strain curves of a bilayer specimen (iRUM-s on iRUM-d) using film-laminated-on-thin-elastomer method³⁷ further confirmed the elastic behavior, along with negligible residue strain and low hysteresis (Supplementary Fig. 62).

Conclusions

In summary, we have successfully demonstrated that covalently-embedded in-situ rubber matrix (iRUM) formation is a simple, effective and widely applicable molecular design approach to simultaneously achieve mechanical robustness, photo-patternability and high electrical performance for polymer electronic materials. The core idea is the excellent miscibility guided by polymer physics principles, combined with elegantly controlled composite film morphology built on the beauty of azide chemistry, i.e. its different reactivities with C-H and C=C bonds. Our iRUM approach results in the *first* intrinsically elastic semiconductor whose charge carrier mobility is comparable to that of amorphous Si and further increase is possible with other recently reported high mobility polymers. Additionally, the developed materials are compatible with solution-processed multilayer device fabrication and can be incorporated into future complex integrated circuits. The iRUM strategy is also promising for mass production when considering the cost-effectiveness and scalability of precursors as well as the reduced cost of expensive active materials resulting from the high content of iRUM (~50 %-75 %). In addition to the transistors demonstrated in this work, the vertical uniformity of iRUMsemiconductor film (Supplementary Fig. 16 to 20) opens up potential applications in vertical electronic devices such as organic light-emitting diodes and organic photovoltaics. The highly accessible and reactive double bonds in iRUM films further provide unique opportunities for pre- and/or post-modification and interfacial engineering through chemical functionalization. This work constitutes a milestone in molecular-level design for the transition from soft/stretchable to elastic and multifunctional skin-inspired electronics.

References

1. Yang, J. C. et al. Electronic Skin: Recent Progress and Future Prospects for Skin-Attachable Devices

- for Health Monitoring, Robotics, and Prosthetics. Adv. Mater. 31, 1904765 (2019).
- 2. Rogers, J. A., Someya, T. & Huang, Y. Materials and Mechanics for Stretchable Electronics. *Science* (80-.). 327, 1603–1607 (2010).
- 3. Kaltenbrunner, M. *et al.* An ultra-lightweight design for imperceptible plastic electronics. *Nature* **499**, 458–463 (2013).
- 4. Lipomi, D. J. & Bao, Z. Stretchable and ultraflexible organic electronics. MRS Bull. 42, 93–97 (2017).
- 5. Bao, Z. Skin-inspired organic electronic materials and devices. MRS Bull. 41, 897–904 (2016).
- 6. Wang, S., Oh, J. Y., Xu, J., Tran, H. & Bao, Z. Skin-Inspired Electronics: An Emerging Paradigm. *Acc. Chem. Res.* **51**, 1033–1045 (2018).
- 7. Zhao, Y. *et al.* Melt-Processing of Complementary Semiconducting Polymer Blends for High Performance Organic Transistors. *Adv. Mater.* **29**, 1605056 (2017).
- 8. Sirringhaus, H. 25th anniversary article: Organic field-effect transistors: The path beyond amorphous silicon. *Adv. Mater.* **26**, 1319–1335 (2014).
- 9. Freudenberg, J., Jänsch, D., Hinkel, F. & Bunz, U. H. F. Immobilization Strategies for Organic Semiconducting Conjugated Polymers. *Chem. Rev.* **118**, 5598–5689 (2018).
- 10. Kim, J. H. *et al.* Understanding mechanical behavior and reliability of organic electronic materials. *MRS Bull.* **42**, 115–123 (2017).
- 11. Root, S. E., Savagatrup, S., Printz, A. D., Rodriquez, D. & Lipomi, D. J. Mechanical Properties of Organic Semiconductors for Stretchable, Highly Flexible, and Mechanically Robust Electronics. *Chem. Rev.* **117**, 6467–6499 (2017).
- 12. Xie, R., Colby, R. H. & Gomez, E. D. Connecting the Mechanical and Conductive Properties of Conjugated Polymers. *Adv. Electron. Mater.* **4**, 1–14 (2018).
- 13. Ashizawa, M., Zheng, Y., Tran, H. & Bao, Z. Intrinsically stretchable conjugated polymer semiconductors in field effect transistors. *Prog. Polym. Sci.* **100**, 101181 (2020).
- 14. Zheng, Y. *et al.* An Intrinsically Stretchable High-Performance Polymer Semiconductor with Low Crystallinity. *Adv. Funct. Mater.* **29**, 1905340 (2019).
- 15. Heinrich, G., Straube, E. & Helmis, G. Rubber elasticity of polymer networks: Theories. in *Polymer Physics* 33–87 (Springer Berlin Heidelberg, 1988).
- 16. Wang, S. *et al.* Skin electronics from scalable fabrication of an intrinsically stretchable transistor array. *Nature* **555**, 83–88 (2018).
- 17. Liu, J. *et al.* Fully stretchable active-matrix organic light-emitting electrochemical cell array. *Nat. Commun.* **11**, 3362 (2020).
- 18. Kim, M. J. *et al.* Universal three-dimensional crosslinker for all-photopatterned electronics. *Nat. Commun.* **11**, 1520 (2020).
- 19. Kwon, H. J. *et al.* Facile Photo-cross-linking System for Polymeric Gate Dielectric Materials toward Solution-Processed Organic Field-Effect Transistors: Role of a Cross-linker in Various Polymer Types. *ACS Appl. Mater. Interfaces* **12**, 30600–30615 (2020).
- 20. Wang, G.-J. N. *et al.* Inducing Elasticity through Oligo-Siloxane Crosslinks for Intrinsically Stretchable Semiconducting Polymers. *Adv. Funct. Mater.* **26**, 7254–7262 (2016).
- 21. Wang, G.-J. N. *et al.* Tuning the Cross-Linker Crystallinity of a Stretchable Polymer Semiconductor. *Chem. Mater.* **31**, 6465–6475 (2019).
- 22. Xu, J. *et al.* Highly stretchable polymer semiconductor films through the nanoconfinement effect. *Science* (80-.). **355**, 59–64 (2017).
- 23. Zhang, G. et al. Versatile Interpenetrating Polymer Network Approach to Robust Stretchable

- Electronic Devices. Chem. Mater. 29, 7645–7652 (2017).
- 24. Guan, Y.-S. *et al.* Air/water interfacial assembled rubbery semiconducting nanofilm for fully rubbery integrated electronics. *Sci. Adv.* **6**, eabb3656 (2020).
- 25. Kong, D. *et al.* Capacitance Characterization of Elastomeric Dielectrics for Applications in Intrinsically Stretchable Thin Film Transistors. *Adv. Funct. Mater.* **26**, 4680–4686 (2016).
- 26. Liu, L. H. & Yan, M. Perfluorophenyl azides: New applications in surface functionalization and nanomaterial synthesis. *Acc. Chem. Res.* **43**, 1434–1443 (2010).
- 27. Png, R. Q. *et al.* High-performance polymer semiconducting heterostructure devices by nitrenemediated photocrosslinking of alkyl side chains. *Nat. Mater.* **9**, 152–158 (2010).
- 28. Young, M. J. T. & Platz, M. S. Mechanistic analysis of the reactions of (pentafluorophenyl)nitrene in alkanes. *J. Org. Chem.* **56**, 6403–6406 (1991).
- 29. Poe, R., Schnapp, K., Young, M. J. T., Grayzar, J. & Platz, M. S. Chemistry and Kinetics of Singlet (Pentafluorophenyl)nitrene. *J. Am. Chem. Soc.* **114**, 5054–5067 (1992).
- 30. Cao, Z., Zhou, Q., Jie, S. & Li, B.-G. High cis -1,4 Hydroxyl-Terminated Polybutadiene-Based Polyurethanes with Extremely Low Glass Transition Temperature and Excellent Mechanical Properties. *Ind. Eng. Chem. Res.* **55**, 1582–1589 (2016).
- 31. Nikzad, S. *et al.* Inducing Molecular Aggregation of Polymer Semiconductors in a Secondary Insulating Polymer Matrix to Enhance Charge Transport. *Chem. Mater.* **32**, 897–905 (2020).
- 32. Kumaraswamy, G. Thermodynamics of high polymer solutions. *Resonance* **22**, 415–426 (2017).
- 33. Lee, J. H., Chung, J. Y. & Stafford, C. M. Effect of confinement on stiffness and fracture of thin amorphous polymer films. *ACS Macro Lett.* **1**, 122–126 (2012).
- 34. Kim, J.-H. et al. Tensile testing of ultra-thin films on water surface. Nat. Commun. 4, 2520 (2013).
- 35. Zhang, S. *et al.* Probing the Viscoelastic Property of Pseudo Free-Standing Conjugated Polymeric Thin Films. *Macromol. Rapid Commun.* **39**, 1800092 (2018).
- 36. Zheng, Y. *et al.* Tuning the Mechanical Properties of a Polymer Semiconductor by Modulating Hydrogen Bonding Interactions. *Chem. Mater.* **32**, 5700–5714 (2020).
- 37. Song, R. *et al.* Unveiling the Stress–Strain Behavior of Conjugated Polymer Thin Films for Stretchable Device Applications. *Macromolecules* **53**, 1988–1997 (2020).
- 38. Sheiko, S. S. & Dobrynin, A. V. Architectural Code for Rubber Elasticity: From Supersoft to Superfirm Materials. *Macromolecules* **52**, 7531–7546 (2019).
- 39. Venkateshvaran, D. *et al.* Approaching disorder-free transport in high-mobility conjugated polymers. *Nature* **515**, 384–388 (2014).
- 40. Mun, J. *et al.* Effect of Nonconjugated Spacers on Mechanical Properties of Semiconducting Polymers for Stretchable Transistors. *Adv. Funct. Mater.* **28**, 1804222 (2018).
- 41. Mun, J. *et al.* Conjugated Carbon Cyclic Nanorings as Additives for Intrinsically Stretchable Semiconducting Polymers. *Adv. Mater.* **31**, 1903912 (2019).
- 42. Oh, J. Y. *et al.* Intrinsically stretchable and healable semiconducting polymer for organic transistors. *Nature* **539**, 411–415 (2016).
- 43. Shin, M. *et al.* Polythiophene nanofibril bundles surface-embedded in elastomer: A route to a highly stretchable active channel layer. *Adv. Mater.* **27**, 1255–1261 (2015).
- 44. Sy Piecco, K. W. E. *et al.* Reusable Chemically Micropatterned Substrates via Sequential Photoinitiated Thiol–Ene Reactions as a Template for Perovskite Thin-Film Microarrays. *ACS Appl. Electron. Mater.* **1**, 2279–2286 (2019).
- 45. Yuk, H., Zhang, T., Lin, S., Parada, G. A. & Zhao, X. Tough bonding of hydrogels to diverse non-

- porous surfaces. Nat. Mater. 15, 190–196 (2016).
- 46. Wang, B. *et al.* High- k Gate Dielectrics for Emerging Flexible and Stretchable Electronics. *Chem. Rev.* **118**, 5690–5754 (2018).
- 47. Wang, Y. *et al.* Polymer-Based Gate Dielectrics for Organic Field-Effect Transistors. *Chem. Mater.* **31**, 2212–2240 (2019).
- 48. Dai, Y., Hu, H., Wang, M., Xu, J. & Wang, S. Stretchable transistors and functional circuits for human-integrated electronics. *Nat. Electron.* (2021) doi:10.1038/s41928-020-00513-5.
- 49. Ji, D., Donner, A. D., Wilde, G., Hu, W. & Fuchs, H. Poly(sodium-4-styrene sulfonate) (PSSNa)-assisted transferable flexible, top-contact high-resolution free-standing organic field-effect transistors. *RSC Adv.* **5**, 98288–98292 (2015).

Acknowledgements

This work was supported by Air Force Office of Scientific Research (Grant No. FA9550-18-1-0143). Part of this work was performed at the Stanford Nano Shared Facilities (SNSF), supported by the National Science Foundation under Award ECCS-2026822. GIXD measurement was carried out at the Stanford Synchrotron Radiation Laboratory (SSRL), SLAC National Accelerator Laboratory, supported by the U.S. Department of Energy, Office of Basic Energy Sciences. S.Z. and X.G. thank financial support from NSF (DMR-2047689) for enabling the thin film mechanics characterization.

Author contributions

Y.Z. and Z.B. conceived the idea. Z.B. directed the project. Y.Z. designed the experiments, conducted key material characterizations, device fabrications and testing. Z.Y. designed key molecular structures and performed syntheses, NMR, FTIR. S.Z., N.P. and X.G. performed measurements and rationales on thin-film mechanics and AFM-IR. X.K., W.M. and J.Q. conducted the MD simulations and rationales. W.W. helped with fully-patterned transistor array fabrication. G.C. performed XPS. D.L. helped with DPPTT syntheses. J.L. and D.Z. helped with mechanical tests. W.Z. and I.M. provided IDTBT semiconductor. S.N. helped with part of GIXD. C.B.C. and J.M. helped with part of AFM measurements. J.K. helped with key rationales and discussions. Y.Z., Z.Y., J.B.-H.T. and Z.B. co-wrote and revised the manuscript.

Competing interests

The authors declare no competing interests.

Data and materials availability

All data are available in the manuscript or Supplementary Information.